

# Revisiting the pro-oxidant activity of copper: interplay of ascorbate, cysteine and glutathione

Enrico Falcone,<sup>a\*</sup> Francesco Stellato,<sup>b,c</sup> Bertrand Vileno,<sup>a</sup> Merwan Bouraguba,<sup>a</sup> Vincent Lebrun,<sup>a</sup>  
Marianne Ilbert,<sup>d</sup> Silvia Morante<sup>b,c</sup> and Peter Fallner<sup>a,e</sup>

<sup>a</sup> *Institut de Chimie (UMR 7177), University of Strasbourg – CNRS, 4 Rue Blaise Pascal, 67081 Strasbourg, France*

<sup>b</sup> *Università di Roma Tor Vergata, Via della Ricerca Scientifica 1 - 00133 Roma, Italy*

<sup>c</sup> *INFN, Sezione di Roma Tor Vergata, Via della Ricerca Scientifica 1 - 00133 Roma, Italy*

<sup>d</sup> *Aix-Marseille Université, CNRS, BIP, UMR 7281, IMM, 31 Chemin Aiguier, 13009 Marseille, France*

<sup>e</sup> *Institut Universitaire de France (IUF), 1 rue Descartes, 75231 Paris, France*

## Abstract

Copper (Cu) is essential for most organisms, but it can be poisonous in excess, through mechanisms such as protein aggregation, trans-metallation and oxidative stress. Latter could implicate the formation of potentially harmful Reactive Oxygen Species (ROS:  $O_2^{\cdot-}$ ,  $H_2O_2$  and  $HO^{\cdot}$ ) via the redox cycling between Cu(II)/Cu(I) states in the presence of dioxygen and physiological reducing agents such as ascorbate (AscH), cysteine (Cys) and the tripeptide glutathione (GSH). Although the reactivity of Cu with these reductants has been previously investigated, the reactions taking place in a more physiologically-relevant mixture of these biomolecules are not known. Hence, we report here on the reactivity of Cu with binary and ternary mixtures of AscH, Cys and GSH. By measuring ascorbate and thiol oxidation, as well as  $HO^{\cdot}$  formation, we show that Cu reacts preferentially with GSH and Cys, halting AscH oxidation and also  $HO^{\cdot}$  release. This could be explained by the formation of Cu-thiolate clusters with both GSH and, as we first demonstrate here, Cys. Moreover, we observed a remarkable acceleration of Cu-catalysed GSH oxidation in the presence of Cys. We provide evidence that both thiol-disulfide exchange and the generated  $H_2O_2$  contribute to this effect. Based on these findings, we speculate that Cu-induced oxidative stress may be mainly driven by GSH depletion and/or protein disulfide formation rather than by  $HO^{\cdot}$  and envision a synergistic effect of Cys on Cu toxicity.

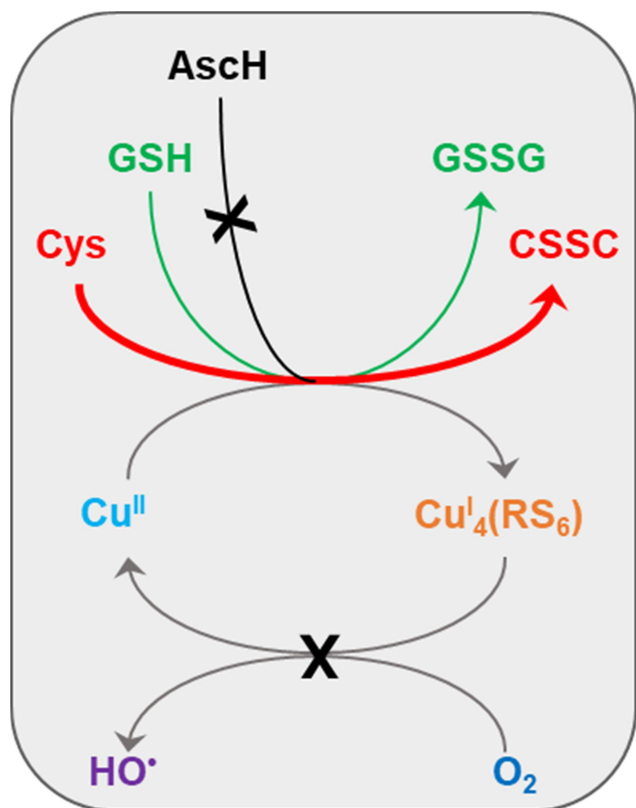
---

\* corresponding author

email: [enrico.falcone@nottingham.ac.uk](mailto:enrico.falcone@nottingham.ac.uk)

current address: School of Chemistry, University of Nottingham, University Park, NG7 2RD Nottingham, UK

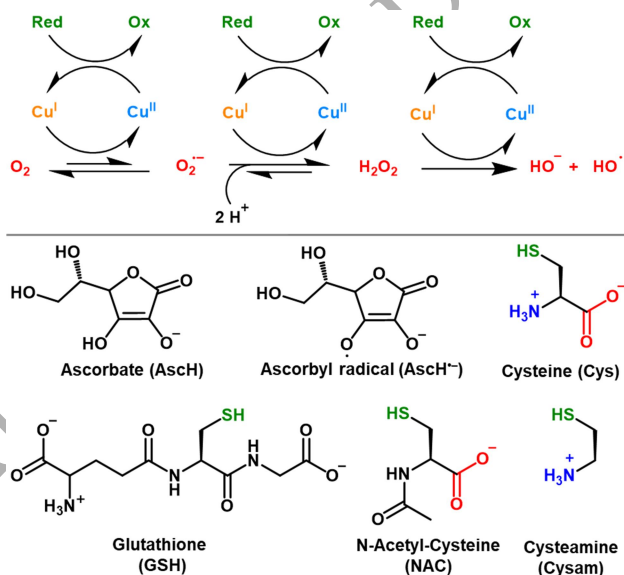
## Graphical Abstract



ORIGINAL UNEDITED MANUSCRIPT

## Introduction

Copper (Cu) is involved in fundamental biochemical processes (e.g. cellular respiration) and hence is an essential element for most organisms. In humans, Cu mostly serves as a redox cofactor of enzymes catalysing the activation of oxygen (e.g. oxidases and monooxygenases) via its cycling between  $\text{Cu}^{\text{I}}$  and  $\text{Cu}^{\text{II}}$  redox states.[1] To prevent undesired Cu redox activity outside the active sites of Cu-enzymes, a set of extracellular carriers, membrane transporter and cytosolic Cu-chaperones ensure a safe Cu transport in the body. Such transporters stabilize Cu in one of the possible redox states, notably  $\text{Cu}^{\text{II}}$  in the oxidizing extracellular milieu and  $\text{Cu}^{\text{I}}$  in the reducing intracellular environment.[2] Nevertheless, their “Cu-buffering” capacity can be overcome in the case of Cu overload, eventually resulting in Cu toxicity. Along with the recently identified trans-metallation of Fe-S clusters and protein aggregation,[3–7] the aerobic redox chemistry of labile (i.e. loosely-bound) Cu, which can lead to the formation of potentially harmful Reactive Oxygen Species (ROS, such as  $\text{O}_2^{\cdot-}$ ,  $\text{H}_2\text{O}_2$  and  $\text{HO}^{\cdot}$ , Scheme 1) and oxidative stress, has been commonly considered accountable for Cu toxicity.[8] Among ROS,  $\text{HO}^{\cdot}$  radical is considered to be one of the most dangerous, due to its higher intrinsic reactivity and to the absence of specific scavenging systems, which instead exist for  $\text{O}_2^{\cdot-}$  (i.e. superoxide dismutase, SOD) and  $\text{H}_2\text{O}_2$  (catalase).[9] Cu-catalysed ROS generation can be fuelled by different physiological reducing agents (Scheme 1), such as ascorbate (AscH), glutathione (GSH) and cysteine (Cys).



**Scheme 1.** *Top*) Mechanism of Cu-catalysed ROS production in the presence of dioxygen and a reducing agent (Red), which is converted to its oxidized form (Ox). *Bottom*) Possible reducing agents in cells are Ascorbate (AscH), Glutathione (GSH) and Cysteine (Cys), which are converted into Ascorbyl radical (AscH $^{\cdot}$ ), Glutathione Disulfide (GSSG) and Cystine (CSSC), respectively. N-acetyl-Cysteine (NAC) and cysteamine (Cysam) are Cys analogues.

AscH is present up to millimolar concentration in cells and is very competent in inducing Cu-catalysed ROS formation in the test tube.[10,11]

GSH is the most abundant thiol in cells (1-10 mM), where it helps keep Cu in the reduced  $\text{Cu}^{\text{I}}$  state.[12] In the test tube, GSH binds  $\text{Cu}^{\text{I}}$  in relatively redox-stable Cu-thiolate clusters, and in cells, it binds labile Cu in the case of overload.[13–15] In contrast, cysteine (Cys, Scheme 1), which reacts with Cu faster than GSH,[16] is found at much lower concentrations (30-250  $\mu\text{M}$ ) and becomes toxic at higher levels.[17]

Although the behaviour of Cu with each of the above-mentioned reductants has been investigated, little is known about the reactions taking place in a more physiologically-relevant mixture of these biomolecules. Therefore, we explored the reactivity of Cu with binary and ternary mixtures of the above-mentioned biomolecules, with the aim to speculate about the possible mechanisms behind Cu-induced oxidative stress.

## Results and discussion

### *Impact of thiols on Cu-catalysed ascorbate oxidation and hydroxyl radical generation*

First, we assessed the effect of thiols on Cu-catalysed aerobic ascorbate oxidation, which can be monitored photometrically via the decrease of its characteristic absorption at 265 nm. Unless otherwise stated, reactions were performed in open microplates, ensuring the availability of dioxygen (dissolved concentration of about 270  $\mu\text{M}$ ). In the absence of thiols, the addition of  $\text{Cu}^{\text{II}}$  promptly triggered the aerobic oxidation of AscH (Fig. 1), which is complete within ~50 min. When GSH was present (at a concentration equal to AscH, 100  $\mu\text{M}$ ) before Cu addition, the onset of AscH oxidation appeared to be remarkably delayed (Fig. 1, green). We supposed, in agreement with the literature,[18] that during such a lag phase Cu catalysed the aerobic oxidation of GSH to GSSG. Indeed, the quantification of GSH through the classical DTNB assay (also known as Ellmann's test) showed that (in the absence of AscH)  $\text{Cu}^{\text{II}}$  was able to catalyse the aerobic oxidation of GSH in a timespan (~180 min) similar to the lag phase observed in the ascorbate oxidation (Fig S1, green).<sup>†</sup> Cys also delayed the onset of Cu-catalysed AscH oxidation, despite to a much lesser extent (~5 min) compared to GSH, which is coherent with the very much faster  $\text{Cu}^{\text{II}}$ -catalysed oxidation of Cys compared to GSH (Fig. 1 and S1, red).[16] Actually, such an inhibitory effect of thiols on Cu-catalysed ascorbate oxidation has been long known,[18–22] and can be interpreted considering that  $\text{Cu}^{\text{II}}$  is first reduced and coordinated by the thiols, where it is stabilized in the  $\text{Cu}^{\text{I}}$  state, and catalyses their oxidation to disulfide by  $\text{O}_2$ , while it catalyses the oxidation of AscH only once little or no reduced thiols are present. Interestingly, when both Cys and GSH were present, the lag phase in AscH oxidation was much shorter than in the absence of Cys (Fig. 1, blue), suggesting that Cys accelerates GSH oxidation, as we also

<sup>†</sup> The results show that GSH oxidation to GSSG is independent of the presence of AscH, indicating that AscH is not catalysing GSH oxidation. Indeed, the steadiness of AscH could have been only apparent, and notably due to a fast reduction of the ascorbyl radical ( $\text{AscH}^{\cdot}$ ) by GSH.[47] This appears to be at most negligible in light of the very similar kinetics of thiols oxidation in the absence and in the presence of ascorbate.

observed in the absence of AscH (Fig. S1, blue). Remarkably, such acceleration is also observed with 10-fold less Cys (100  $\mu$ M) than GSH (1 mM), which are in the range of physiological concentrations (Fig. S2).

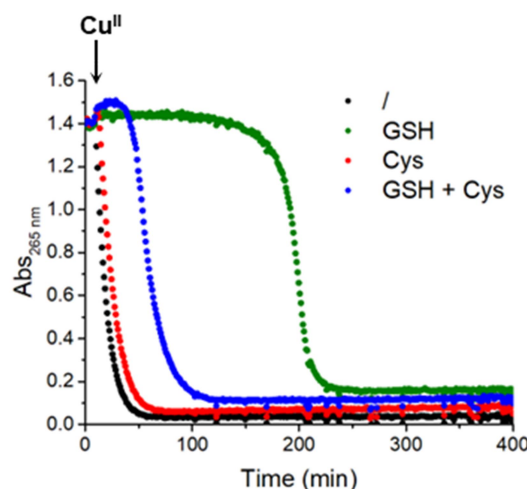


**Figure 1.** Effect of thiols on  $\text{Cu}^{\text{II}}$ -catalysed oxidation of AscH. Ascorbate oxidation in the presence of  $\text{Cu}^{\text{II}}$  only (black),  $\text{Cu}^{\text{II}}$  and GSH (green),  $\text{Cu}^{\text{II}}$  and Cys (red),  $\text{Cu}^{\text{II}}$ , GSH and Cys (blue); conditions:  $[\text{AscH}] = 100 \mu\text{M}$ ,  $[\text{Cu}^{\text{II}}] = 10 \mu\text{M}$ ,  $[\text{GSH}] = 100 \mu\text{M}$ ,  $[\text{Cys}] = 100 \mu\text{M}$ , phosphate buffer 50 mM pH 7.4.

Since Cu-catalysed aerobic oxidation of ascorbate and thiols is normally accompanied by the formation of ROS (Scheme 1), we also followed the  $\text{HO}^\bullet$  production using CCA (Coumarin-Carboxylic Acid), which forms the fluorescent 7-hydroxy-CCA ( $\lambda_{\text{ex}} = 390 \text{ nm}$ ,  $\lambda_{\text{em}} = 452 \text{ nm}$ ) upon reaction with  $\text{HO}^\bullet$ . Interestingly, no  $\text{HO}^\bullet$  was detected as long as reduced thiols were present (Fig. S3A). Noteworthy, the time delay observed for the onset of  $\text{HO}^\bullet$  production fits that of the beginning of AscH oxidation. Moreover, although no  $\text{HO}^\bullet$  was detected in the presence of Cys only (Fig. S3B), the latter was oxidised too fast to significantly delay the  $\text{HO}^\bullet$  production in the presence of AscH. Of note, the measurement of TEMPOL (4-hydroxy-2,2,6,6-tetramethylpiperidin-1-oxyl) EPR signal, which is quenched by reaction with  $\text{HO}^\bullet$ , also showed that no significant amount of  $\text{HO}^\bullet$  is produced by  $\text{Cu}^{\text{II}}$  in the presence of thiols (Fig. S3C).

#### *Spectroscopic evidence for the formation of Cu-Cys clusters*

In order to explain why the Cu-catalysed GSH oxidation by  $\text{O}_2$  does not generate  $\text{HO}^\bullet$  radicals, it has been suggested that GSH-bound  $\text{Cu}^{\text{I}}$  reduces  $\text{H}_2\text{O}_2$  to  $\text{H}_2\text{O}$ , rather than  $\text{HO}^\bullet$ .<sup>[23]</sup> This process is indeed plausible, especially in light of the currently-known formation of multinuclear  $\text{Cu}_x(\text{GS})_y$  clusters,<sup>[13]</sup> where the proximity of several Cu ions could favour the occurrence of a two-electron reduction. Since  $\text{Cu}^{\text{II}}$  did not produce  $\text{HO}^\bullet$  in the presence of Cys, we assessed whether Cu-thiolate clusters are also formed with Cys by means of X-ray absorption spectroscopy (XAS) and low-temperature luminescence.

Both the Cu K-edge XANES (X-ray Absorption Near Edge Spectroscopy) and EXAFS (Extended X-ray Absorption Fine Structure) spectra (Fig. 2) of Cu-Cys and Cu-GSH samples are indistinguishable within the experimental error. Therefore, the Cu coordination in Cu-Cys is

substantially identical to that in Cu-GSH, which forms mostly  $\text{Cu}_4(\text{GS})_6$  clusters.[13] Indeed, the EXAFS data can be fitted by a model  $\text{Cu}_4\text{S}_6$  cluster,[24,25] in which each Cu atom is surrounded by 3 S atoms at about 2.3 Å and a “disordered” shell (i.e. with relatively high values of  $\sigma^2$ , the mean square deviation of the distance) composed of 3 Cu atoms at about 2.8 Å (Fig. S4 and Table S1), although models with a different number of Cu scatterers cannot be ruled out solely based on EXAFS data.

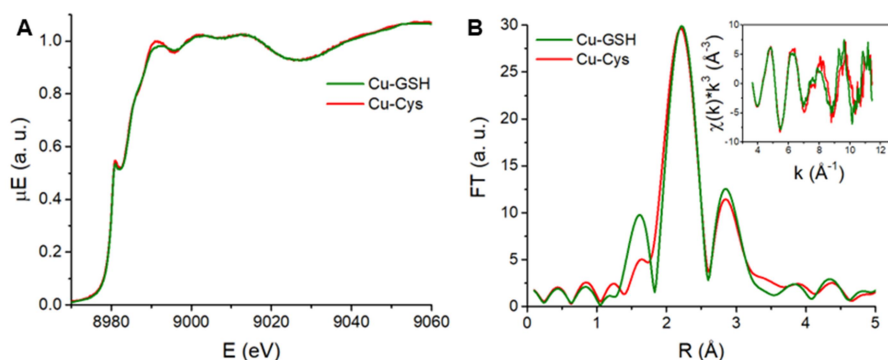


**Figure 2.** XANES spectra (A) and Fourier Transforms (B) of the EXAFS (inset) spectra of Cu-GSH (green) and Cu-Cys (red) complexes. Conditions:  $[\text{Cu}^{\text{II}}] = 1 \text{ mM}$ ,  $[\text{GSH}] = 10 \text{ mM}$ ,  $[\text{Cys}] = 10 \text{ mM}$ , phosphate buffer 200 mM pH 7.4.

In light of the known luminescent emission of  $\text{Cu}_4(\text{GS})_6$  and Cu-metallothioneins clusters,[13,26] we also recorded low-temperature (77 K) luminescence spectra of Cu-Cys and Cu-GSH. Interestingly, upon excitation at 310 nm, Cu-Cys exhibited a luminescent emission band at 418 nm, similar but slightly blue-shifted compared to the emission of Cu-GSH at 423 nm (Figure 3A), attributed to tetranuclear  $\text{Cu}_4(\text{GS})_6$ . Likewise, the excitation spectrum ( $\lambda_{\text{em}} = 310 \text{ nm}$ ) of Cu-Cys appears to be blue-shifted compared to that of Cu-GSH (Figure 3B), in agreement with the absorption spectra reported in the literature.[13,27] This further confirms that, similarly to GSH, Cu and Cys form tetranuclear  $\text{Cu}_4(\text{Cys})_6$  clusters. In addition, we measured the luminescence of a mixture of Cu, GSH and Cys, which showed emission and excitation spectra very similar to those of Cu-GSH clusters, suggesting that GSH has a higher affinity for Cu than Cys. Notwithstanding, the accelerating effect of Cys on GSH oxidation suggests that a minor portion of Cu-Cys or mixed Cu-GSH/Cys clusters exist.

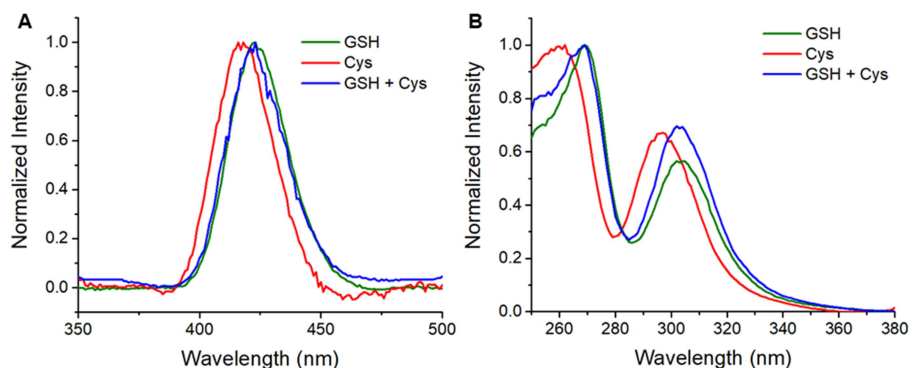


**Figure 3.** Low-temperature (77 K) luminescence emission (A) and excitation (B) spectra of Cu-thiols mixtures (GSH, green; Cys, red; GSH and Cys, blue). Conditions:  $[\text{Cu}^{\text{II}}] = 100 \mu\text{M}$ ,  $[\text{GSH}] = 1 \text{ mM}$ ,  $[\text{Cys}] = 1 \text{ mM}$ , phosphate buffer 50 mM pH 7.4.

*Insights into the mechanism of Cys-accelerated GSH oxidation*

Previous reports have shown the acceleration of GSH oxidation by Cys in the absence of Cu or the presence of Cu,Zn-SOD, and the thiol-disulfide exchange reaction between cysteine disulfide, CSSC, and GSH (Eq. 1) has been postulated as the mechanism.[28–30]



To assess such a hypothesis, we compared the kinetics of GSH oxidation by  $\text{Cu}^{\text{II}}$  in the presence of Cys and CSSC using the lag phase in AsCh oxidation assay as a convenient read-out for the thiol oxidation kinetics. Indeed, if CSSC accelerates GSH oxidation simply via thiol-disulfide exchange, a shorter lag phase (of less than  $\sim 5$  min in our conditions, i.e. the time needed to completely oxidise Cys to CSSC) would be expected when directly adding the corresponding amount (0.5 equivalent, i.e.  $50 \mu\text{M}$ ) of CSSC, rather than Cys, to the mixture containing AsCh, GSH and  $\text{Cu}^{\text{II}}$ . Actually, although CSSC accelerated GSH oxidation, the lag phase proved to be longer when  $50 \mu\text{M}$  CSSC, rather than  $100 \mu\text{M}$  Cys, was added (Fig. 4, orange), suggesting that the catalytic effect of Cys on GSH oxidation is not merely driven by the thiol-disulfide exchange between CSSC and GSH. Considering that  $\text{H}_2\text{O}_2$  is also formed along Cys oxidation to CSSC,[31] we explored the possibility that  $\text{H}_2\text{O}_2$  also contributes to the acceleration of GSH oxidation. Indeed, the addition of  $50 \mu\text{M}$   $\text{H}_2\text{O}_2$  together with  $50 \mu\text{M}$  CSSC (Fig. 4, gold), decreased the lag phase more than CSSC alone, and notably to a very similar extent compared to  $100 \mu\text{M}$  Cys (Fig. 4, blue). Therefore, along with the thiol-disulfide exchange previously suggested, the  $\text{H}_2\text{O}_2$  produced during Cys oxidation by  $\text{Cu}^{\text{II}}$  seems to contribute to the acceleration of GSH oxidation. Interestingly, the Cu/Cys-catalysed aerobic GSH oxidation could contribute to Cys toxicity and also exacerbate the toxicity of excess Cu in cells.

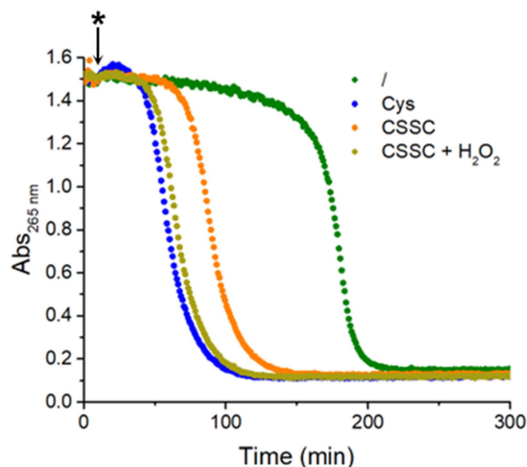


**Figure 4.** Effect of CSSC and  $\text{H}_2\text{O}_2$  on the  $\text{Cu}^{\text{II}}$ -catalysed oxidation of AscH in the presence of GSH. Conditions:  $[\text{AscH}] = 100 \mu\text{M}$ ,  $[\text{Cu}^{\text{II}}] = 10 \mu\text{M}$ ,  $[\text{GSH}] = 100 \mu\text{M}$ ,  $[\text{Cys}] = 100 \mu\text{M}$ ,  $[\text{CSSC}] = 50 \mu\text{M}$ ,  $[\text{H}_2\text{O}_2] = 50 \mu\text{M}$ , phosphate buffer 50 mM pH 7.4. First, AscH and GSH were pre-mixed; then, at the time point indicated by \*, the following compounds were added:  $\text{Cu}^{\text{II}}$  (green),  $\text{Cu}^{\text{II}}$  and Cys (blue),  $\text{Cu}^{\text{II}}$  and CSSC (orange),  $\text{Cu}^{\text{II}}$ , CSSC and  $\text{H}_2\text{O}_2$  (gold).

To better understand the faster oxidation of Cys compared to GSH and its accelerating effect, we also examined the reactivity of its derivatives N-Acetyl-Cysteine (NAC, Scheme 1), which is commonly used as an antioxidant,[32] and cysteamine (Cysam, Scheme 1), a simple aminothiols. Thus, we assessed the effect of NAC and Cysam on the GSH oxidation in the presence of  $\text{Cu}^{\text{II}}$  using the AscH oxidation assay (Fig. 5 and S5).  $\text{Cu}^{\text{II}}$ -catalysed aerobic NAC oxidation also appeared to be faster than GSH oxidation (Fig. 5, magenta), but to a much lower extent than for Cys. Instead, Cysam reacted, at least, as fast as Cys (Fig. S5). However, contrary to Cys and Cysam (Fig. S5), NAC had little (if at all) impact on the rate of GSH oxidation (Fig. 5, violet). Such faster oxidation of Cys, Cysam and NAC compared to GSH could be explained by their ability to chelate  $\text{Cu}^{\text{II}}$  in a bidentate fashion via the thiol group together with the amino (Cys and Cysam) or carboxylate (NAC) moiety (Scheme 1). Indeed, since the re-oxidation of  $\text{Cu}^{\text{I}}$  to  $\text{Cu}^{\text{II}}$  is considered the rate-limiting step of the Cu-catalysed thiol oxidation,[16] the stabilization of the  $\text{Cu}^{\text{II}}$  state by Cys, Cysam and NAC can fasten the reaction. Besides, the negligible effect of NAC on the rate of GSH oxidation can be attributed to its higher  $\text{pK}_a$  (9.5) compared to Cys (8.3) and Cysam (8.2), which implies a much slower thiol-disulfide exchange.[33,34]



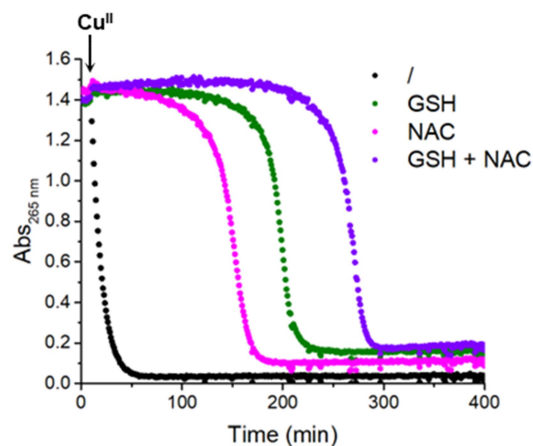


**Figure 5.** Effect of NAC on GSH oxidation. Ascorbate oxidation in the presence of  $\text{Cu}^{\text{II}}$  (black),  $\text{Cu}^{\text{II}}$  and GSH (green),  $\text{Cu}^{\text{II}}$  and NAC (magenta) or  $\text{Cu}^{\text{II}}$ , GSH and NAC (violet); conditions:  $[\text{AscH}] = 100 \mu\text{M}$ ,  $[\text{Cu}^{\text{II}}] = 10 \mu\text{M}$ ,  $[\text{GSH}] = 100 \mu\text{M}$ ,  $[\text{NAC}] = 100 \mu\text{M}$ , phosphate buffer 50 mM pH 7.4.

## Conclusions

Excess labile copper is generally considered to be toxic owing, among other mechanisms, to the formation of ROS through  $\text{O}_2$  reduction by  $\text{Cu}^{\text{I}}$  ions. Hence, Cu-catalysed ROS production depends primarily on dioxygen (whose level in cells can vary quite a lot, from normoxic, to hypoxic such as in cancer, down to zero in cells living anaerobically) and reducing agents. In cells, the most relevant Cu reductants are ascorbate, GSH or Cys. In this study, we confirm that in a mixture of such biomolecules, oxidation of the two thiols occurs before that of ascorbate. Interestingly, the spectrophotometric measurement of ascorbate concentration at 265 nm results to be a convenient *in-situ* readout of thiol oxidation. Importantly, and in line with the literature,[23] Cu-catalysed aerobic GSH/Cys oxidation is not accompanied by the release of harmful  $\text{HO}^\bullet$  radicals, which are instead detected during Cu-catalysed aerobic ascorbate oxidation. It is worth noting that this behaviour is not an intrinsic feature of thiols, as  $\text{HO}^\bullet$  can be detected when thiol oxidation is catalysed by Cu-complexes.[35] Hence, we speculate that such reactivity of thiols arises from the formation of Cu-thiolate clusters. Indeed, we showed that Cys also forms tetranuclear Cu-S clusters similar to the already known  $\text{Cu}_4(\text{GS})_6$ . [13] Interestingly, the proximity of several Cu ions in a multinuclear cluster could favour the two-electron reduction of  $\text{H}_2\text{O}_2$  to  $\text{H}_2\text{O}$  that was suggested by previous studies.[23] Alternatively,  $\text{HO}^\bullet$  radicals could be formed by Cu-GSH/Cys but react with the neighbouring thiols of the cluster, preventing their release and detection by external probes (CCA or TEMPOL in this study). Hence, the potential role of Cu-thiolate clusters in preventing  $\text{HO}^\bullet$  formation or release is worthy of further experimental and computational investigations. Besides, in analogy with previous reports,[28–30] we observed that Cys, as well as Cysam but not NAC, accelerates Cu-catalysed GSH oxidation, although Cu-GSH is the predominant species even in the presence of equimolar Cys. We also showed that GSH oxidation is accelerated even at physiologically relevant sub-

stoichiometric Cys:GSH ratio of 1:10. Moreover, not only thiol-disulfide exchange but also oxidation via  $\text{H}_2\text{O}_2$  contribute to the Cu-catalysed acceleration of GSH oxidation by Cys.

From a biological perspective, our findings suggest that, in the case of Cu overload, oxidative stress arises, in the first instance, from aberrant disulfide, notably GSSG, formation, rather than  $\text{HO}^\bullet$  production. It is indeed well established that excess Cu promotes GSH depletion, altering the GSH/GSSG balance.[15,36–38] Although this impairs cellular redox homeostasis, excess Cu buffering by GSH helps to protect other potential Cu targets, such as protein thiols. Indeed, upon GSH depletion, Cys-containing proteins with high Cu-affinity (e.g. those containing the CXXC motif)[39] could undergo Cu-catalysed oxidation resulting in loss of function. Moreover, as recently demonstrated, Cu can also target protein thiols in compartments such as bacterial periplasm, where GSH concentration is lower.[40,41] Furthermore, in light of the recent discovery of lipoylated proteins as preferential targets of Cu toxicity,[6] the ability of Cu to catalyse lipoic acid (a dithiol) oxidation despite the presence of excess GSH remains to be assessed. Whether Cu-catalysed protein disulfide formation is accompanied by  $\text{HO}^\bullet$  formation is another important aspect that warrants future studies. Interestingly, the ability of Cu to oxidize and hence deplete Cys faster than GSH, could be one of the reasons why, during evolution, an N-protected thiol like GSH, rather than an aminothiols like Cys, was selected as the most abundant intracellular thiol: GSH represents a more resilient Cu buffering system than Cys, ensuring longer protection and survival in the case of Cu stress. Finally, it is noteworthy that, as it has been shown for Fe,[42] high Cys levels may exacerbate the poisonous effects of excess Cu ions on cellular redox homeostasis, and hence the increase of Cys levels can be envisioned as a strategy to enhance the cytotoxic activity of Cu for therapeutic purposes.

### Acknowledgements

We thank Dr Gabriele Meloni (UT Dallas) and Dr Olivier Proux (ESRF, Grenoble) for help with luminescence and XAS measurements, respectively. E.F. acknowledges financial support from the French National Research Agency (ANR) through the CHAPCOP-ANR-19-CE44-0018 program. S.M. and F.S. acknowledge financial support from the University of Rome Tor Vergata through the PANDA project and from the INFN through the BIOPHYS initiative.

## Materials and methods

### Stock solutions

Commercially available chemicals were used without further purification. All stock solutions were prepared in ultrapure water ( $\rho = 18.2 \text{ M}\Omega\cdot\text{cm}^{-1}$ ).  $\text{Cu}^{\text{II}}$  stock solution was prepared by dissolving  $\text{CuCl}_2\cdot 2\text{H}_2\text{O}$  salt and its concentration was assessed by UV-vis absorption at 780 nm ( $\epsilon_{780} = 12 \text{ M}^{-1}\text{cm}^{-1}$ ). A stock solution of the phosphate buffer (pH 7.4) was prepared by mixing  $\text{KH}_2\text{PO}_4$  and  $\text{K}_2\text{HPO}_4$  and adjusting the pH with a concentrated solution of NaOH. Solutions of sodium ascorbate, GSH, Cys and NAC were freshly prepared before the experiments. Cysteamine stock solution was prepared as follows: cysteamine hydrochloride powder was flushed with  $\text{N}_2$ , then dissolved in 1 mM HCl thoroughly flushed with  $\text{N}_2$  and stored at  $-20^\circ\text{C}$ . The concentration of cysteamine was determined via the DTNB assay (see below).

### Ascorbate oxidation assay

Ascorbate oxidation was monitored by absorption at 265 nm on a CLARIOstar (BMG Labtech) plate reader inside an open 96-well microplate (Greiner) or in a closed cuvette using an Agilent Cary 60 spectrophotometer (Fig. S2). After mixing AscH (100  $\mu\text{M}$ ) and thiols (100  $\mu\text{M}$  each) in phosphate buffer (50 mM, pH 7.4), the signal was monitored for about 10 min to assure no ascorbate auto-oxidation was taking place. Then,  $\text{Cu}^{\text{II}}$  (10  $\mu\text{M}$ ) was added and the reaction was monitored over time.

### DTNB assay

Thiols oxidation was measured upon the reaction of reduced thiols with the Ellmann's reagent, 5,5'-dithio-bis-(2-nitrobenzoic acid) (DTNB), monitoring the formation of the  $\text{TNB}^{2-}$  product by absorption at 412 nm on a CLARIOstar plate reader inside a 96-well microplate (Greiner). After mixing  $\text{Cu}^{\text{II}}$  (10  $\mu\text{M}$ ) and thiols (100  $\mu\text{M}$  each) in phosphate buffer (50 mM, pH 7.4), aliquots (25-50  $\mu\text{l}$ ) were taken at several time points and transferred to the assay mixture (final volume 100  $\mu\text{l}$ ) containing 100  $\mu\text{M}$  DTNB and 1 mM EDTA in 50 mM TRIS buffer pH 8.2 (final concentration of thiol being 50  $\mu\text{M}$ ). Thiol concentration was calculated using  $\epsilon_{412} = 14150 \text{ M}^{-1}\text{cm}^{-1}$ .

### CCA assay

The formation of 7-hydroxy-coumarin-3-carboxylic acid (7-OH-CCA) was monitored by fluorescence emission at 452 nm upon excitation at 390 nm on a CLARIOstar plate reader inside a 96-well microplate (Greiner).  $\text{Cu}^{\text{II}}$  (10  $\mu\text{M}$ ) was added to a solution containing CCA (500  $\mu\text{M}$ ) and AscH, thiols or their mixture (each at 100  $\mu\text{M}$ ) in phosphate buffer (50 mM, pH 7.4) and the reaction was monitored over time.

### EPR spin scavenging

EPR spin scavenging experiments were performed at room temperature ( $T = 295 \pm 1\text{K}$ ) using an EMX-plus (Bruker Biospin GmbH, Germany) X-band EPR spectrometer equipped with a high sensitivity resonator (4119HS-W1, Bruker). Samples were introduced into glass capillaries (Hirschmann, 25  $\mu\text{L}$ ) sealed at both ends and rapidly transferred into the EPR cavity for measurement. The principal experimental parameters were microwave frequency of  $\sim 9.8\text{ GHz}$ , microwave power of  $\sim 4.5\text{ mW}$ , modulation amplitude 1 G, time constant of  $\sim 5\text{ ms}$ , conversion time of  $\sim 12.5\text{ ms}$ . A scan (sweeping time of  $\sim 10\text{ s}$ ) was then acquired every 17 s to obtain the kinetics of TEMPOL reduction over time. All spectra were best simulated and the resulting simulations were doubly integrated to relatively quantify the concentration of remaining TEMPOL ( $I/I_0 = I(t)/I(t=0)$ ). Data analysis and simulations based on experimental data were performed using Xenon (Bruker Biospin GmbH, Germany) and lab-made routines based on EasySpin Toolbox under Matlab (Mathworks) environment.[43]

### XAS

XAS data at the Cu K-edge were acquired at the BM30 beamline of the European Synchrotron Radiation Facility (ESRF - Grenoble, France). The beamline energy was calibrated using a metallic Cu foil by setting the position of the absorption edge (defined as the first maximum of the first derivative curve) to 8979 eV. Spectra were recorded in fluorescence mode using a 13-element solid-state Ge detector. In order to minimize X-ray-induced damage, the samples were kept at 10 K in a He cryostat throughout the measurements. The ATHENA software[44] was used to normalize XANES data and to extract the EXAFS signal, which was obtained by cubic splines interpolation as implemented in the AUTOBK algorithm.[45] The quantitative analysis of the EXAFS spectra was performed using the EXCURV98 code.[46]

### Low-temperature luminescence

Low-temperature luminescence spectra were recorded using a FluoroMax Plus spectrofluorometer (Horiba Scientific) equipped with a cylindrical quartz dewar filled with liquid nitrogen (at 77 K). 500  $\mu\text{l}$  samples were transferred to quartz tubes with 4 mm inner diameter and freeze-quenched into liquid nitrogen before their introduction in the dewar.

### **Data Availability**

Data available on request.

## References

1. Festa RA, Thiele DJ. Copper: An essential metal in biology. *Curr Biol* 2011;**21**:R877–83.
2. Rubino JT, Franz KJ. Coordination chemistry of copper proteins: How nature handles a toxic cargo for essential function. *J Inorg Biochem* 2012;**107**:129–43.
3. Macomber L, Imlay JA. The iron-sulfur clusters of dehydratases are primary intracellular targets of copper toxicity. *Proc Natl Acad Sci U S A* 2009;**106**:8344–9.
4. Wiebelhaus N, Zaengle-Barone JM, Hwang KK, Franz KJ, Fitzgerald, MC. Protein Folding Stability Changes across the Proteome Reveal Targets of Cu Toxicity in *E. coli*. *ACS Chem Biol* 2021;**16**:214–24.
5. Robison ATR, Sturrock GR, Zaengle-Barone JM, Wiebelhaus N, Dharani A, Williams IG, Fitzgerald MC, Franz KJ. Analysis of copper-induced protein precipitation across the *E. coli* proteome. *Metallomics* 2023;**15**, DOI: 10.1093/mtomes/mfac098.
6. Tsvetkov P, Coy S, Petrova B, Dreishpoon M, Verma A, Abdusamad M, Rossen J, Joesch-Cohen L, Humeidi R, Spangler RD, Eaton JK, Frenkel E, Kocak M, Corsello SM, Lutsenko S, Kanarek N, Santagata S, Golub TR. Copper induces cell death by targeting lipoylated TCA cycle proteins. *Science* 2022;**375**:1254–61.
7. Zuily L, Lahrach N, Fassler R, Genest O, Faller P, Sénèque O, Denis Y, Castanié-Cornet MP, Genevaux P, Jakob U, Reichmann D, Giudici-Orticoni MT, Ilbert, M. Copper Induces Protein Aggregation, a Toxic Process Compensated by Molecular Chaperones. *MBio* 2022;**13**, DOI: 10.1128/mbio.03251-21.
8. Jomova K, Valko M. Advances in metal-induced oxidative stress and human disease. *Toxicology* 2011;**283**:65–87.
9. He L, He T, Farrar S, Ji L, Liu T, Ma X. Antioxidants Maintain Cellular Redox Homeostasis by Elimination of Reactive Oxygen Species. *Cell Physiol Biochem* 2017;**44**:532–53.
10. Rice ME. Ascorbate regulation and its neuroprotective role in the brain. *Trends Neurosci* 2000;**23**:209–16.
11. Buettner GR, Jurkiewicz BA. Catalytic metals, ascorbate and free radicals: Combinations to avoid. *Radiat Res* 1996;**145**:532–41.
12. Schafer FQ, Buettner GR. Redox environment of the cell as viewed through the redox state of the glutathione disulfide/glutathione couple. *Free Radic Biol Med* 2001;**30**:1191–212.
13. Morgan MT, Nguyen LAH, Hancock HL, Fahrni CJ. Glutathione limits aquacopper(I) to sub-femtomolar concentrations through cooperative assembly of a tetranuclear cluster. *J Biol Chem* 2017;**292**:21558–67.
14. Morgan MT, Bourassa D, Harankhedkar S, McCallum AM, Zlatic SA, Calvo JS, Meloni G, Faundez V, Fahrni CJ. Ratiometric two-photon microscopy reveals attomolar copper buffering in normal and Menkes mutant cells. *Proc Natl Acad Sci* 2019;**116**:12167–72.
15. Stewart LJ, Ong CLY, Zhang MM, Brouwer S, McIntyre L, Davies MR, Walker MJ, McEwan AG, Waldron KJ, Djoko KY. Role of Glutathione in Buffering Excess Intracellular Copper in *Streptococcus pyogenes*. *MBio* 2020;**11**:1–19.
16. Smith RC, Reed VD, Hill WE. Oxidation of thiols by copper(II). *Phosphorus Sulfur Silicon Relat Elem* 1994;**90**:147–54.
17. Osman LP, Mitchell SC, Waring RH. Cysteine, its Metabolism and Toxicity. *Sulfur reports* 1997;**20**:155–72.
18. Carrasco-Pozo C, Aliaga ME, Olea-Azar C, Speisky H. Double edge redox-implications for

the interaction between endogenous thiols and copper ions: In vitro studies. *Bioorg Med Chem* 2008;**16**:9795–803.

19. Frederick Gowland Hopkins B, James Morgan E. Some relations between ascorbic acid and glutathione. *Biochem J* 1936;**30**:1446.

20. Gould IA. Protective Influence of Glutathione on Copper-Induced Oxidation of Ascorbic Acid in Milk. *J Dairy Sci* 1940;**23**:991–6.

21. Ionescu JG, Poljsak B. Metal ions mediated pro-oxidative reactions with vitamin c: Possible implications for treatment of different malignancies. *Cancer Prev Res Perspect* 2011;**3**:149–82.

22. Du YT, Long Y, Tang W, Liu XF, Dai F, Zhou B. Prooxidative inhibition against NF- $\kappa$ B-mediated inflammation by pharmacological vitamin C. *Free Radic Biol Med* 2022;**180**:85–94.

23. Spear N, Aust SD. Hydroxylation of deoxyguanosine in DNA by copper and thiols. *Arch Biochem Biophys* 1995;**317**:142–8.

24. Dance IG, Bowmaker GA, Clark GR, Seadon JK. The formation and crystal and molecular structures of hexa( $\mu$ -organothiolato)tetracuprate(I) cage dianions: bis-(tetramethylammonium)hexa-( $\mu$ -methanethiolato)tetracuprate(I) and two polymorphs of bis(tetramethylammonium)hexa-( $\mu$ -benzenethiolato)-tetracuprate(I). *Polyhedron* 1983;**2**:1031–43.

25. Pickering IJ, George GN, Dameron CT, Kurz B, Winge DR, Dance IG. X-ray Absorption Spectroscopy of Cuprous-Thiolate Clusters in Proteins and Model Systems. *J Am Chem Soc* 1993;**115**:9498–505.

26. Pountney DL, Schauwecker I, Zarn J, Vařák M. Formation of Mammalian Cu8-Metallothionein in Vitro: Evidence for the Existence of Two Cu(I)4-Thiolate Clusters. *Biochemistry* 1994;**33**:9699–705.

27. Pecci L, Montefoschi G, Musci G, Cavallini D. Novel findings on the copper catalysed oxidation of cysteine. *Amino Acids* 1997;**13**:355–67.

28. Winterbourn CC, Peskin A V., Parsons-Mair HN. Thiol oxidase activity of copper,zinc superoxide dismutase. *J Biol Chem* 2002;**277**:1906–11.

29. Bakavayev S, Chetrit N, Zvagelsky T, Mansour R, Vyazmensky M, Barak Z, Israelson A, Engel S. Cu/Zn-superoxide dismutase and wild-type like fALS SOD1 mutants produce cytotoxic quantities of H<sub>2</sub>O<sub>2</sub> via cysteine-dependent redox short-circuit. *Sci Rep* 2019;**9**:1–13.

30. Hogg N. The effect of cyst(e)ine on the auto-oxidation of homocysteine. *Free Radic Biol Med* 1999;**27**:28–33.

31. Kachur A V., Koch CJ, Biaglow JE. Mechanism of copper-catalyzed autoxidation of cysteine. *Free Radic Res* 1999;**31**:23–34.

32. Zhitkovich A. N-Acetylcysteine: Antioxidant, Aldehyde Scavenger, and More. *Chem Res Toxicol* 2019;**32**:1318–9.

33. Whitesides GM, Lilburn JE, Szajewski RP. Rates of Thiol-Disulfide Interchange Reactions between Mono and Dithiols and Ellman's Reagent. *J Org Chem* 1977;**42**:332–8.

34. Nagy P. Kinetics and mechanisms of thiol-disulfide exchange covering direct substitution and thiol oxidation-mediated pathways. *Antioxidants Redox Signal* 2013;**18**:1623–41.

35. Falcone E, Ritacca AG, Hager S, Schueffl H, Vileno B, El Khoury Y, Hellwig P, Kowol CR, Heffeter P, Sicilia E, Faller P. Copper-catalysed glutathione oxidation is accelerated by the anticancer thiosemicarbazone Dp44mT and further boosted at lower pH. *J Am Chem Soc* 2022;**144**:14758–14768.

36. Stoiber TL, Shafer MM, Perkins DAK, Hemming JDC, Armstrong DE. Analysis of glutathione endpoints for measuring copper stress in *Chlamydomonas reinhardtii*. *Environ*

*Toxicol Chem* 2007;**26**:1563.

37. Hultberg M, Isaksson A, Andersson A, Hultberg B. Traces of copper ions deplete glutathione in human hepatoma cell cultures with low cysteine content. *Chem Biol Interact* 2007;**167**:56–62.
38. García-Fernández AJ, Bayoumi AE, Pérez-Pertejo Y, Motas M, Reguera RM, Ordóñez C, Balaña-Fouce R, Ordóñez D. Alterations of the glutathione-redox balance induced by metals in CHO-K1 cells. *Comp Biochem Physiol C Toxicol Pharmacol* 2002;**132**:365–73.
39. Brose J, La Fontaine S, Wedd AG, Xiao Z. Redox sulfur chemistry of the copper chaperone Atox1 is regulated by the enzyme glutaredoxin 1, the reduction potential of the glutathione couple GSSG/2GSH and the availability of Cu(i). *Metallomics* 2014;**6**:793–808.
40. Eben SS, Imlay JA. Excess copper catalyzes protein disulfide bond formation in the bacterial periplasm but not in the cytoplasm. *Mol Microbiol* 2023, DOI: 10.1111/mmi.15032.
41. Hiniker A, Collet J-F, Bardwell JCA. Copper Stress Causes an in Vivo Requirement for the Escherichia coli Disulfide Isomerase DsbC. *J Biol Chem* 2005;**280**:33785–91.
42. Park S, Imlay JA. High levels of intracellular cysteine promote oxidative DNA damage by driving the Fenton reaction. *J Bacteriol* 2003;**185**:1942–50.
43. Stoll S, Schweiger A. EasySpin, a comprehensive software package for spectral simulation and analysis in EPR. *J Magn Reson* 2006;**178**:42–55.
44. Ravel B, Newville M. ATHENA, ARTEMIS, HEPHAESTUS: Data analysis for X-ray absorption spectroscopy using IFEFFIT. *J Synchrotron Radiat* 2005;**12**:537–41.
45. Newville M, Livin P, Yacoby Y, Rehr JJ, Stern EA. Near-edge x-ray-absorption fine structure of Pb: A comparison of theory and experiment. *Phys Rev B* 1993;**47**:14126–31.
46. Binsted N, Gurman SJ, Campbell JW. Daresbury Laboratory {EXCURV}98 Program. *CLRC Daresbury Lab Warringt* 1998.
47. Winkler BS, Orselli SM, Rex TS. The redox couple between glutathione and ascorbic acid: a chemical and physiological perspective. *Free Radic Biol Med* 1994;**17**:333–49.

ORIGINAL UNEDITED MANUSCRIPT